JACS
JOURNAL OF THE AMERICAN CHEMICAL SOCIETY

Article

pubs.acs.org/JACS

From Highly Crystalline to Outer Surface-Functionalized Covalent Organic Frameworks—A Modulation Approach

Mona Calik,[‡] Torben Sick,[‡] Mirjam Dogru, Markus Döblinger, Stefan Datz, Harald Budde, Achim Hartschuh, Florian Auras, and Thomas Bein*

Department of Chemistry and Center for NanoScience (CeNS), University of Munich (LMU), Butenandtstrasse 5-13, 81377 Munich, Germany

Supporting Information

ABSTRACT: Crystallinity and porosity are of central importance for many properties of covalent organic frameworks (COFs), including adsorption, diffusion, and electronic transport. We have developed a new method for strongly enhancing both aspects through the introduction of a modulating agent in the synthesis. This modulator competes with one of the building blocks during the solvothermal COF growth, resulting in highly crystalline frameworks with greatly increased domain sizes reaching several hundreds of nanometers. The obtained materials feature fully accessible pores with an internal surface area of over 2000 m^2 g^{-1}. Compositional analysis via NMR spectroscopy revealed that the COF-5 structure can form over a wide range of boronic acid-to-catechol ratios, thus producing frameworks with compositions ranging from highly boronic acid-deficient to networks with catechol voids. Visualization of an −SH-functionalized modulating agent via iridium staining revealed that the COF domains are terminated by the modulator. Using functionalized modulators, this synthetic approach thus also provides a new and facile method for the external surface functionalization of COF domains, providing accessible sites for post-synthetic modification reactions. We demonstrate the feasibility of this concept by covalently attaching fluorescent dyes and hydrophilic polymers to the COF surface. We anticipate that the realization of highly crystalline COFs with the option of additional surface functionality will render the modulation concept beneficial for a range of applications, including gas separations, catalysis, and optoelectronics.

INTRODUCTION

Covalent organic frameworks (COFs) represent an emerging class of crystalline, porous materials exhibiting unique structural and functional diversity. By combining multidentate building blocks via covalent bonds, two- or three-dimensional frameworks with defined pore size and high specific surface area in conjunction with appreciable thermal and chemical stability can be constructed.[1,2] Depending on their topology and functionality, these reticular materials are promising candidates for various applications, such as gas adsorption,[3,4] separation,[5,6] catalysis,[7,8] proton conduction,[9] energy storage,[10] and optoelectronics.[11−15]

In the context of the latter applications, COFs consisting of two-dimensional layers (2D COFs) are of particular interest. These frameworks are realized by combining virtually planar building units into extended two-dimensional sheets, which assemble via dispersive forces (π-stacking) into highly anisotropic porous, crystalline materials. While the topology of a COF can be predesigned via the geometry of its building blocks, the actual formation of a long-range ordered network relies on the reversibility of the covalent bond formation. Only if the reaction conditions are chosen such that the covalent bonds can be formed, broken, and re-formed at a sufficiently high rate, thus providing a functional "self-healing" mechanism, will crystalline frameworks be obtained. COF syntheses have predominantly been realized through reversible condensation reactions, including the formation of B−O bonds (boroxines, boronate esters,[16−18] and borosilicates[19]), imines,[20,21] imides,[22,23] and others.[24−26]

While the optimization of the COF growth conditions can produce fairly crystalline frameworks, the realization of particularly well-ordered COFs with large domain sizes requires an even higher degree of synthetic control.

The effects of ligands on the nucleation, growth, and properties of materials have been studied extensively for metal[27] and inorganic semiconductor nanocrystals.[28,29] Also, nanoparticles of coordination polymers have been modified by the addition of surfactants and capping agents.[30] In the field of metal−organic frameworks (MOFs), modulation concepts, which utilize the competition between the bridging ligands and a mono-functionalized terminating ligand, have proven very successful. Enabling the adjustment of growth kinetics and energies of specific crystal facets via selection of the modulator, this approach has been demonstrated to allow for the growth of highly crystalline MOFs with tailored morphology and domain sizes.[31−34]

Received: October 13, 2015
Published: December 22, 2015

DOI: 10.1021/jacs.5b10708
J. Am. Chem. Soc. 2016, 138, 1234−1239

Dichtels's group recently demonstrated that 3D COFs can be functionalized internally by adding truncated building blocks bearing functional groups to the synthesis mixture.[35−37] Growth rates of 2D COFs have been studied depending on the monomer reactivity and solvent mixtures.[38−40]

In this work, we transfer the modulation concept to the synthesis of a 2D COF. Applying monoboronic acids as modulators in the solvothermal synthesis of the archetypical COF-5, we are able to influence and optimize the crystallinity, domain size, and porosity of the resulting framework. Moreover, the addition of phenylboronic acids bearing a functional group opens up a novel, convenient way for the surface functionalization of COF crystallites, which can be used for subsequent modifications, such as the attachment of dyes or polymers.

RESULTS AND DISCUSSION

The hexagonal COF-5 was synthesized via a microwave-assisted co-condensation of 2,3,6,7,10,11-hexahydroxytriphenylene (HHTP) with 1.5 equiv of benzene-1,4-diboronic acid (BDBA) in a 1:1 solvent mixture of mesitylene and 1,4-dioxane (Figure 1). When a modulating agent was used in the synthesis, 2 equiv of the modulator (denoted as COF-5-*x*, where *x* is expressed in %) was substituted for a fraction *x* of BDBA, thus keeping the amount of boronic acid groups in the reaction mixture constant. In our study the degree of substitution was systematically varied from 0 to 70%.

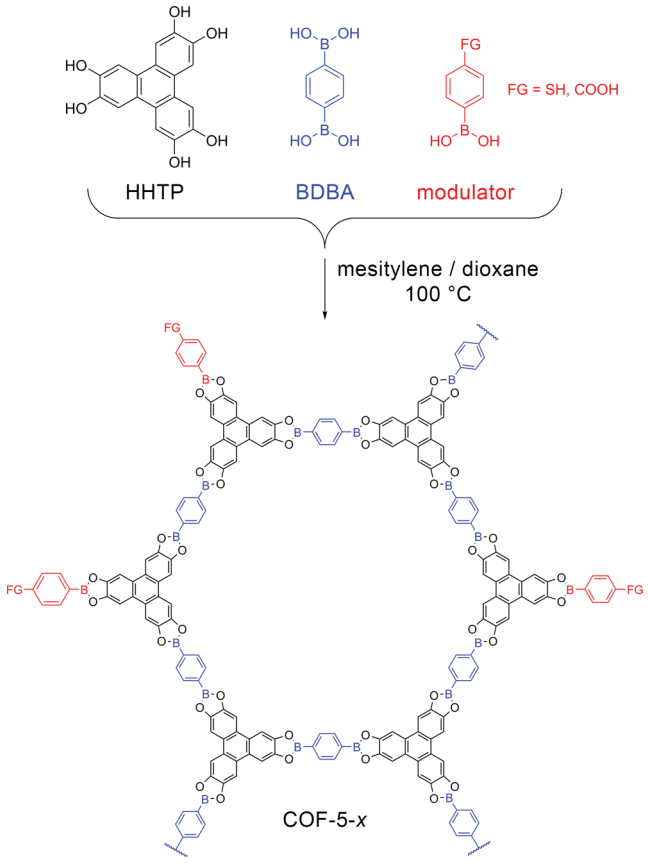

Figure 1. Synthesis of COF-5-*x* via a co-condensation reaction of benzene-1,4-diboronic acid (blue) and 2,3,6,7,10,11-hexahydroxytriphenylene (black) in the presence of a modulating agent (red) bearing a functional group.

As a first example for a modulating agent, we chose 4-mercaptophenylboronic acid (MPBA), as its size, shape, and solubility are similar to those of BDBA. Additionally, its thiol group provides a way of detecting the incorporated modulator (see below).

The influence of the modulator on the COF-5 crystallinity was monitored by powder X-ray diffraction (PXRD) analysis (Figure 2a). Successful formation of the COF-5 framework was observed up to $x = 60$. We found that the introduction of small amounts of the modulating agent led to an enhanced crystallinity of the resulting COF, as evidenced by a sharpening of the reflections. The COF-5-5 and COF-5-10 samples exhibit a series of particularly sharp reflections and a number of higher-order reflections, indicating the presence of large crystalline domains with a very low concentration of defects (Supporting Information (SI), Figure S6). The XRD patterns can be indexed assuming a hexagonal *P6/mmm* symmetry (Figures 2b and S4a). Small deviations from this idealized model, i.e., a tilt of the bridging phenyl groups ($P\bar{3}$, Figure S4b) or a serrated rather than a fully eclipsed layer arrangement (*Cmcm*, Figure S4c), would produce nearly identical patterns and thus cannot be identified on the basis of the experimental data (Figure S5). Pawley refinement of the experimental data applying the *P6/mmm*-symmetric model produced lattice parameters of $a = b = 2.98 \pm 0.02$ nm and $c = 0.35 \pm 0.01$ nm.

COF-5 has been reported to be highly porous with a Brunauer−Emmett−Teller (BET) surface area of up to 1590 $m^2\ g^{-1}$ and a pore volume of 0.998 $cm^3\ g^{-1}$ (Figure 2c).[1] Nitrogen sorption experiments carried out for the COF-5-*x* series reveal a close correlation of the surface area and pore volume with the crystallinity of the frameworks (Figure 2d,e). While in our hands the modulator-free synthesis produced frameworks with a surface area of 1200 $m^2\ g^{-1}$ and a pore volume of 0.64 $cm^3\ g^{-1}$, the substitution of the modulator for 10% of the BDBA increased the surface area to 2100 $m^2\ g^{-1}$ at a pore volume of 1.14 $cm^3\ g^{-1}$. This represents an increase of 32% in surface area when compared to literature values and 75% when compared to our own data for the modulator-free COF-5-0. Moreover, these values are close to the theoretical Connolly surface area and pore volume (2130 $m^2\ g^{-1}$ and 1.21 $cm^3\ g^{-1}$, respectively), indicating the realization of a highly crystalline network with fully open and accessible pores. Furthermore, the distinct step in the sorption isotherms at $p/p_0 = 0.1$ underlines the very well-defined porosity of this material.[41−43] A further increase of the modulator content above $x = 10$ led to a gradual decrease in surface area and pore volume. The shape of the obtained isotherms also changes upon the substitution. COF-5-0 and the COF-5-10 exhibit the typical sharp increase at $p/p_0 = 0.1$ that is caused by the simultaneous pore condensation in the uniformly sized pores. The samples grown at a higher modulator concentration, COF-5-25, COF-5-50, and COF-5-60, however, display an increasingly broadened slope, suggesting less uniform pores and an increasing contribution of textural porosity. This trend is also reflected in the corresponding pore size distributions determined by quenched solid density functional theory (QSDFT) calculations (Figure S11).

Transmission electron microscopy (TEM) images of the COF grown at several modulator contents underline the influence of the MPBA on the resulting material. While COF-5-0 is composed of intergrown domains that are 30−50 nm in size (Figure 3a), the domains of COF-5-10 can extend to hundreds of nanometers (Figure 3b). Depending on

DOI: 10.1021/jacs.5b10708
J. Am. Chem. Soc. 2016, 138, 1234−1239

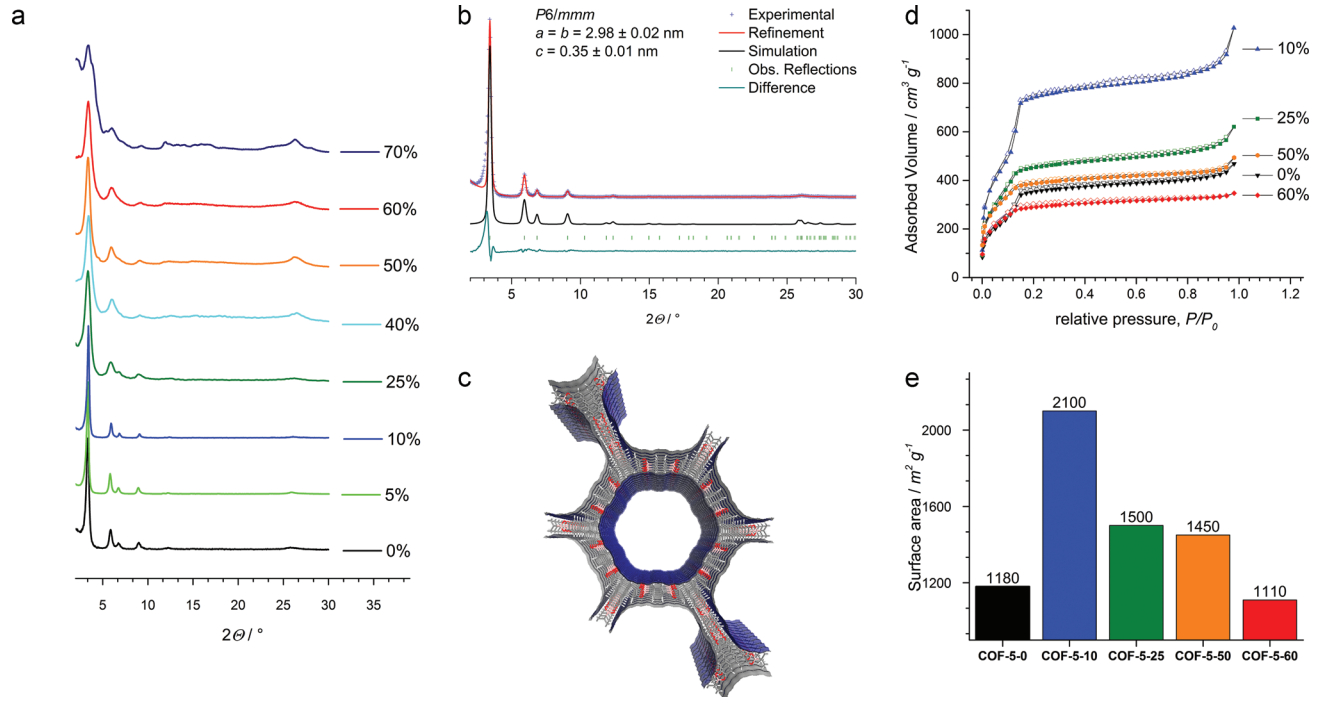

Figure 2. (a) Comparison of the PXRD patterns of the COF-5-*x* series. (b) Pawley refinement assuming *P6/mmm* symmetry (red) of the COF-5-10 PXRD pattern (blue), simulated pattern (black), reflection positions (green) and difference plot (dark green). (c) Illustration of COF-5 showing the hexagonal pores and the Connolly surface (blue). (d) Nitrogen sorption isotherms of the COF-5-*x* series recorded at 77 K. (e) BET surface areas obtained from the nitrogen sorption experiments.

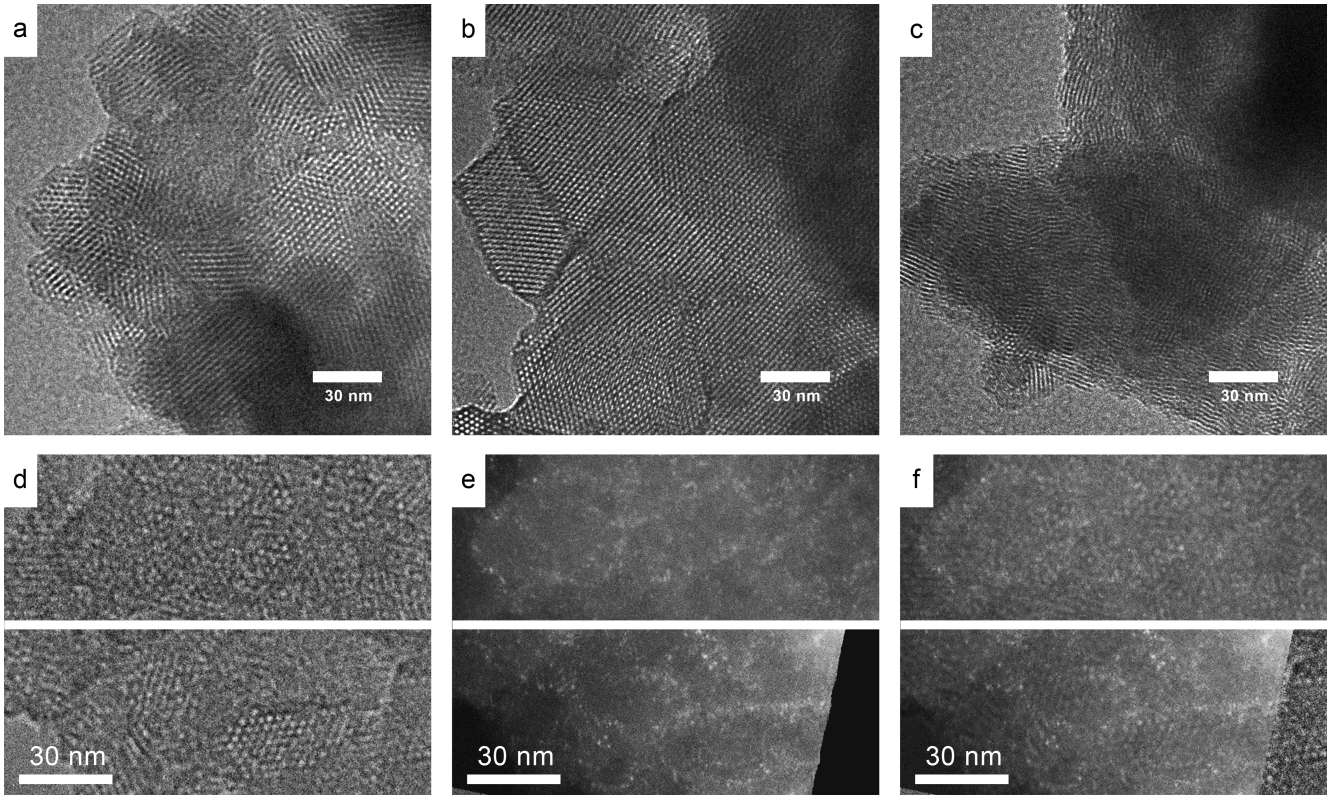

Figure 3. TEM micrographs of (a) COF-5-0, (b) COF-5-10, and (c) COF-5-25. (d)TEM micrographs of COF-5-10 stained with iridium at two different sample positions. (e) Corresponding scanning transmission electron microscopy (STEM) micrographs of the same sample positions. (f) Overlay of TEM and STEM micrographs of COF-5-10 showing the increased Ir occurrence at the grain boundaries of the crystallite domains.

the orientation of a domain, either the hexagonal arrangement of the pores or straight porous channels are visible. Increased content of the modulator results in an apparent deterioration of the structural quality and a decrease of the domain size to only

DOI: 10.1021/jacs.5b10708
J. Am. Chem. Soc. 2016, 138, 1234−1239

15−20 nm for COF-5-25, which we attribute primarily to the depletion of the bridging diboronic acid in the reaction mixture (Figure 3c).

Based on these experimental findings we propose the following mechanism for the modulator-assisted COF growth:

The modulator acts as a capping agent for the developing COF, terminating the 2D sheets during lateral growth. By repetitive attachment and detachment, the modulator slows the COF formation. The COF crystals thus experience an increased number of precipitation and dissolution steps, thus facilitating the healing of defects and bringing the system closer to thermodynamic equilibrium. Moreover, the modulator can saturate point or line defects, such as partially unreacted building blocks and dislocations, thus reducing strain in the crystal and allowing for a more stable overall crystal conformation. Consequently, adding small amounts of the modulator enables the formation of very large and highly crystalline COF domains.

In order to gain further insights into the formation mechanism, we compared the growth kinetics of unmodulated and modulated COF-5 (Figure S9). In the absence of a modulator, the first reflections of the COF appear already after 0.5 h. After 4 h, all of the starting material has been consumed, and the crystallinity increases only moderately over the next 92 h (Figure S9a). If 10% MPBA is used in the synthesis, the COF formation is slowed down appreciably, while the reflections of the starting material disappear faster (Figure S9b). First very weak reflections appear after 1 h, but remain considerably weaker than the corresponding ones of the unmodulated sample for the next hours. Only after 16 h, the same reflection intensity is reached and the crystallinity of the modulated sample outperforms that of the unmodulated sample thereafter. The same trend was also observed for CPBA serving as modulator (Figure S9c).

As the COF formation is thermodynamically favored over the precipitation of oligomers that might block the porous channels, we expect the modulator-assisted synthesis to produce COFs with very high porosity. Indeed, the surface area and pore volume are the highest for the modulator contents that yield the most crystalline COFs. Also, porosity values that are close to the theoretical maximum were achieved without an activation procedure, during which precipitated reactants and oligomers are digested and washed away.

On the basis of the above considerations, some of the modulator is expected to incorporate into the crystal structure at high modulator concentration. For a quantitative compositional analysis, the COF-5 samples grown at different modulator concentrations were dissolved by adding pinacol in deuterated DMSO. The proton NMR signals of HHTP, pinacol-terminated BDBA and the pinacol-terminated modulators (MPBA or CPBA) were found to be sufficiently separated to allow for a quantification of the COF constituents.

For the highly ordered COF-5-x samples ($x \leq 10$) no modulator was detected (Figures S1−S3). As the surface-to-volume ratio is very small for the relatively large domains of COF-5-5 and COF-5-10, the amount of modulator that could be attached to the outer surface would be below the detection limit of this method. Starting from $x = 25$ we observe an increasing incorporation of the modulator into the structure, reaching a BDBA:MPBA ratio of 1:1 for $x = 60$ (Table S4).

The HHTP:BDBA ratio reveals striking deviations from the expected 2:3 molecular composition of the idealized COF-5 structure. In the absence of the modulator, we observe a 6:4.3 ratio of the aryl proton integrals, corresponding to a 1:1.1 molar ratio of the two building blocks. This BDBA deficiency requires a significant amount of voids to be incorporated into the COF structure. Indeed, the pore size distribution of COF-5-0 features an additional contribution of smaller pores around 20 Å (Figure S11).

The composition of COF-5-10, which exhibits the highest degree of order, was found to be very close to the theoretical HHTP:BDBA molar ratio. In line with this observation, this material does not possess any porosity in addition to the hexagonal pore channels.

Further increasing the modulator content in the reaction mixture leads to a gradual decrease of the incorporated BDBA, which is, however, fully balanced by the increasing incorporation of the modulator. The overall HHTP:boronic acid group ratio remains constant at 1:3, indicating that all OH groups were saturated in the framework (Table S4). As the space occupied by the diboronic acid in the framework is too small to accommodate two molecules of the modulator, the observed amount of modulator can only be incorporated alongside with HHTP voids (Figure S12). This would cause additional small pores inside the COF walls, which are indeed observed in the pore size distributions of COF-5-25, -50, and -60 (Figure S11).

In addition to the nonspecific incorporation at high modulator concentration in the synthesis mixture, we expect the modulator, acting as capping agent for the growing crystal domains, to accumulate at grain boundaries. Due to the instability of the framework at large TEM probe currents, a direct determination of the −SH distribution inside the framework via energy-dispersive X-ray (EDX) analysis was not possible. Therefore, an indirect method was chosen, where the −SH groups that are pointing into free space were stained with iridium clusters (Figure S10a) and visualized by scanning TEM in high-angle annular dark-field mode (STEM-HAADF) imaging (for further information see the SI, section 2).[44] In STEM-HAADF images, the intensity distribution is approximately proportional to the square of the atomic number. By overlaying the STEM-HAADF images and TEM images, recorded at the same sample positions, an accumulation of Ir clusters at grain boundaries, with respect to the crystal domains, was observable as white dots (Figure 3d−f). A COF-5-0 sample that does not feature the −SH functionalization did not show any preferred localization of the iridium clusters but a random distribution within the network (Figure S17).

Having studied the effect of substituting an −SH-functionalized modulator for a fraction of the diboronic acid, we wondered whether a similar effect on the COF crystallization was also achievable with phenylboronic acids bearing other functional groups. Introducing carboxyphenyl boronic acid (CPBA) as modulating agent resulted in the same increase in domain size up to $x = 10$ followed by a gradual decrease as the modulator content was increased beyond 10% (Figure S7). The application of the non-functionalized phenylboronic acid as modulator, however, did not produce crystalline COFs, possibly due to a different solubility and polarity.

The above substitution approach proved to be very sensitive to the modulator concentration and led to small domains for $x > 10$, which we attribute primarily to an increasingly unfavorable ratio between the bridging diboronic acid and the terminating monoboronic acid. In order to allow for high modulator contents, thus ensuring optimal reaction control, but at the same time providing enough diboronic acid to form extended networks, we tested the addition of variable amounts

DOI: 10.1021/jacs.5b10708
J. Am. Chem. Soc. 2016, 138, 1234−1239

of the modulating agent to a stoichiometric reaction mixture of HHTP and BDBA. The addition of CPBA to a 2:3 mixture of HHTP and BDBA resulted in improved crystallinity, with the optimal modulator:BDBA ratio being at 3:10 (Figure S8). Highest crystallinity of the COF was achieved at a slightly higher modulator:BDBA ratio than for the substitution approach (i.e., 2:9, corresponding to 10% substitution), while the resulting domain sizes and the general trends were very similar.

Post-functionalization of framework materials typically includes the risk of sample decomposition or the loss of crystallinity. In the case of 2D COFs, the delamination of the π-stacked, and thus comparably weakly interacting layers can be an issue of particular importance. Moreover, sterically demanding functional groups might prove very difficult to incorporate into close-packed 2D COFs and to convert in post-modification reactions. In cases where a modification on the outer surface of a COF domain is sufficient, the use of functionalized modulators during the COF synthesis can provide a convenient and versatile alternative. As discussed above, the modulator is expressed at the outer surface of individual COF crystallites. Thus, the functional group of a para-substituted modulator, such as MPBA or CPBA, will be pointing away from the COF, rendering it easily accessible for subsequent reactions.

As a first example for illustrating this concept, we chose the attachment of a fluorescent dye to the carboxylic acid-functionalized CPBA-modulated COF-5-10 surface. The *N*-ethyl-*N*′-(3-(dimethylamino)propyl)carbodiimide hydrochloride (EDC)-activated −COOH groups were found to react readily at room temperature with the amino-functionalized ATTO 633 dye. Any unreacted, not covalently bound dye was removed by extensive washing prior to the measurements. PXRD measurements confirmed that the crystallinity had been fully retained during this process (Figure S10b). The newly formed amide bond was identified via IR spectroscopy (Figure S13a). Moreover, the presence of the dye was confirmed via UV−Vis diffuse reflectance measurements (Figure S15). While the COF-5-COOH absorbs strongly at wavelengths below 400 nm, its absorption in the visible range is very low and free of spectral features. The attachment of the dye gives rise to an increased absorption between 400 and 600 nm with a distinct absorption feature at 643 nm. The successful attachment of the dye was further confirmed via photoluminescence measurements (Figure S16). Upon excitation with a HeNe laser at 633 nm the ATTO633 modified COF exhibits a broad emission centered at 766 nm. As expected for a dye that is immobilized at a surface, both the absorption and emission spectra are broadened and red-shifted versus the respective spectra of the dye in solution.[45]

This strategy can also be used to coat the COF crystallites with a shell of a different material, thus altering properties like stability, dispersibility, or bio-compatibility. Methoxypolyethylene glycol maleimide (PEG-maleimide) was successfully attached to MPBA-modified COF-5-10 via a Michael-type addition (Figure S13b).[46] While the bare COF-5-*x* is not stable toward alcohols, the PEG-modified material was found to retain its crystallinity upon soaking in ethanol. The corresponding PXRD pattern does not show any loss in crystallinity, whereas the non-functionalized COF-5-10 sample degrades rapidly (Figure S10c).

CONCLUSION

We have developed a modulation strategy for the growth of highly crystalline COFs with large domains and very high porosity. Competition between the bridging COF building block and the terminating modulation agent was found to influence the dynamic equilibrium during framework formation, slowing down the COF growth and supporting the self-healing of crystal defects. Under optimized conditions, the crystal domains of the boronate ester-linked COF-5 reached several hundreds of nanometers. The pores of the framework were found to be open and fully accessible even without any activation procedure, which is reflected by a surface area close to the theoretical maximum and a very narrow pore size distribution.

Compositional analysis via NMR revealed that the COF-5 structure forms over a wide range of molecular compositions, from highly diboronic acid-deficient frameworks to networks comprising an excess of the linear building block.

The use of functionalized modulating agents furthermore provides a new strategy for functionalizing the outer surface of COF crystallites. These functional groups were found to be accessible for the subsequent covalent attachment of molecules or polymers, allowing for further modification of the chemical, physical, or electronic properties of the COF.

The combination of an enhanced degree of crystallinity and the option for an outer surface post-modification of COF domains might prove beneficial for a range of applications, such as gas separation, catalysis, superresolution imaging, and optoelectronics.

ASSOCIATED CONTENT

Supporting Information

The Supporting Information is available free of charge on the ACS Publications website at DOI: 10.1021/jacs.5b10708.

Experimental methods, synthetic procedures, and additional structural and spectroscopic data, including Tables S1−S5 and Figures S1−S17 (PDF)

AUTHOR INFORMATION

Corresponding Author

*bein@lmu.de

Author Contributions

‡M.C. and T.S. contributed equally to this work.

Notes

The authors declare no competing financial interest.

ACKNOWLEDGMENTS

The authors are grateful for funding from the German Science Foundation (DFG; Research Cluster NIM) and the Free State of Bavaria (Research Network SolTech). The research leading to these results has received funding from the European Research Council under the European Union's Seventh Framework Programme (FP7/2007-2013)/ERC Grant Agreement No. 321339.

REFERENCES

(1) Côte, A. P.; Benin, A. I.; Ockwig, N. W.; O'Keeffe, M.; Matzger, A. J.; Yaghi, O. M. *Science* **2005**, *310*, 1166.
(2) Uribe-Romo, F. J.; Hunt, J. R.; Furukawa, H.; Klöck, C.; O'Keeffe, M.; Yaghi, O. M. *J. Am. Chem. Soc.* **2009**, *131*, 4570.
(3) Furukawa, H.; Yaghi, O. M. *J. Am. Chem. Soc.* **2009**, *131*, 8875.

DOI: 10.1021/jacs.5b10708
J. Am. Chem. Soc. 2016, 138, 1234−1239

(4) Doonan, C. J.; Tranchemontagne, D. J.; Glover, T. G.; Hunt, J. R.; Yaghi, O. M. *Nat. Chem.* **2010**, *2*, 235.
(5) Oh, H.; Kalidindi, S. B.; Um, Y.; Bureekaew, S.; Schmid, R.; Fischer, R. A.; Hirscher, M. *Angew. Chem., Int. Ed.* **2013**, *52*, 13219.
(6) Ma, H.; Ren, H.; Meng, S.; Yan, Z.; Zhao, H.; Sun, F.; Zhu, G. *Chem. Commun.* **2013**, *49*, 9773.
(7) Xu, H.; Chen, X.; Gao, J.; Lin, J.; Addicoat, M.; Irle, S.; Jiang, D. *Chem. Commun.* **2014**, *50*, 1292.
(8) Ding, S.-Y.; Gao, J.; Wang, Q.; Zhang, Y.; Song, W.-G.; Su, C.-Y.; Wang, W. *J. Am. Chem. Soc.* **2011**, *133*, 19816.
(9) Chandra, S.; Kundu, T.; Kandambeth, S.; BabaRao, R.; Marathe, Y.; Kunjir, S. M.; Banerjee, R. *J. Am. Chem. Soc.* **2014**, *136*, 6570.
(10) DeBlase, C. R.; Silberstein, K. E.; Truong, T.-T.; Abruña, H. c. D.; Dichtel, W. R. *J. Am. Chem. Soc.* **2013**, *135*, 16821.
(11) Dogru, M.; Handloser, M.; Auras, F.; Kunz, T.; Medina, D.; Hartschuh, A.; Knochel, P.; Bein, T. *Angew. Chem., Int. Ed.* **2013**, *52*, 2920.
(12) Calik, M.; Auras, F.; Salonen, L. M.; Bader, K.; Grill, I.; Handloser, M.; Medina, D. D.; Dogru, M.; Löbermann, F.; Trauner, D.; Hartschuh, A.; Bein, T. *J. Am. Chem. Soc.* **2014**, *136*, 17802.
(13) Medina, D. D.; Werner, V.; Auras, F.; Tautz, R.; Dogru, M.; Schuster, J.; Linke, S.; Döblinger, M.; Feldmann, J.; Knochel, P.; Bein, T. *ACS Nano* **2014**, *8*, 4042.
(14) Feng, X.; Honsho, Y.; Saengsawang, O.; Liu, L.; Wang, L.; Saeki, A.; Irle, S.; Seki, S.; Dong, Y.; Jiang, D. *Adv. Mater.* **2012**, *24*, 3026.
(15) Jin, S.; Ding, X.; Feng, X.; Supur, M.; Furukawa, K.; Takahashi, S.; Addicoat, M.; El-Khouly, M. E.; Nakamura, T.; Irle, S.; Fukuzumi, S.; Nagai, A.; Jiang, D. *Angew. Chem., Int. Ed.* **2013**, *52*, 2017.
(16) Côte, A. P.; El-Kaderi, H. M.; Furukawa, H.; Hunt, J. R.; Yaghi, O. M. *J. Am. Chem. Soc.* **2007**, *129*, 12914.
(17) Spitler, E. L.; Dichtel, W. R. *Nat. Chem.* **2010**, *2*, 672.
(18) Ding, X.; Guo, J.; Feng, X.; Honsho, Y.; Guo, J.; Seki, S.; Maitarad, P.; Saeki, A.; Nagase, S.; Jiang, D. *Angew. Chem., Int. Ed.* **2011**, *50*, 1289.
(19) Hunt, J. R.; Doonan, C. J.; LeVangie, J. D.; Côté, A. P.; Yaghi, O. M. *J. Am. Chem. Soc.* **2008**, *130*, 11872.
(20) Chen, X.; Addicoat, M.; Irle, S.; Nagai, A.; Jiang, D. *J. Am. Chem. Soc.* **2013**, *135*, 546.
(21) Zhang, Y.-B.; Su, J.; Furukawa, H.; Yun, Y.; Gándara, F.; Duong, A.; Zou, X.; Yaghi, O. M. *J. Am. Chem. Soc.* **2013**, *135*, 16336.
(22) Fang, Q.; Zhuang, Z.; Gu, S.; Kaspar, R. B.; Zheng, J.; Wang, J.; Qiu, S.; Yan, Y. *Nat. Commun.* **2014**, *5*, 4503.
(23) Fang, Q.; Wang, J.; Gu, S.; Kaspar, R. B.; Zhuang, Z.; Zheng, J.; Guo, H.; Qiu, S.; Yan, Y. *J. Am. Chem. Soc.* **2015**, *137*, 8352.
(24) Uribe-Romo, F. J.; Doonan, C. J.; Furukawa, H.; Oisaki, K.; Yaghi, O. M. *J. Am. Chem. Soc.* **2011**, *133*, 11478.
(25) Dalapati, S.; Jin, S.; Gao, J.; Xu, Y.; Nagai, A.; Jiang, D. *J. Am. Chem. Soc.* **2013**, *135*, 17310.
(26) Jackson, K. T.; Reich, T. E.; El-Kaderi, H. M. *Chem. Commun.* **2012**, *48*, 8823.
(27) Yu, W. W.; Wang, Y. A.; Peng, X. *Chem. Mater.* **2003**, *15*, 4300.
(28) Leff, D. V.; Ohara, P. C.; Heath, J. R.; Gelbart, W. M. *J. Phys. Chem.* **1995**, *99*, 7036.
(29) Tao, A. R.; Habas, S.; Yang, P. *Small* **2008**, *4*, 310.
(30) Uemura, T.; Kitagawa, S. *Chem. Lett.* **2005**, *34*, 132.
(31) Diring, S.; Furukawa, S.; Takashima, Y.; Tsuruoka, T.; Kitagawa, S. *Chem. Mater.* **2010**, *22*, 4531.
(32) Tsuruoka, T.; Furukawa, S.; Takashima, Y.; Yoshida, K.; Isoda, S.; Kitagawa, S. *Angew. Chem., Int. Ed.* **2009**, *48*, 4739.
(33) Schaate, A.; Roy, P.; Godt, A.; Lippke, J.; Waltz, F.; Wiebcke, M.; Behrens, P. *Chem. - Eur. J.* **2011**, *17*, 6643.
(34) Biemmi, E.; Darga, A.; Stock, N.; Bein, T. *Microporous Mesoporous Mater.* **2008**, *114*, 380.
(35) Bunck, D. N.; Dichtel, W. R. *Angew. Chem., Int. Ed.* **2012**, *51*, 1885.
(36) Bunck, D. N.; Dichtel, W. R. *Chem. Commun.* **2013**, *49*, 2457.
(37) Brucks, S. D.; Bunck, D. N.; Dichtel, W. R. *Polymer* **2014**, *55*, 330.
(38) Smith, B. J.; Dichtel, W. R. *J. Am. Chem. Soc.* **2014**, *136*, 8783.
(39) Smith, B. J.; Hwang, N.; Chavez, A. D.; Novotney, J. L.; Dichtel, W. R. *Chem. Commun.* **2015**, *51*, 7532.
(40) Colson, J. W.; Mann, J. A.; DeBlase, C. R.; Dichtel, W. R. *J. Polym. Sci., Part A: Polym. Chem.* **2015**, *53*, 378.
(41) Sing, K. S. W.; Everett, D. H.; Haul, R. A. W.; Moscou, L.; Pierotti, R. A.; Rouquérol, J.; Siemieniewska, T. *Pure Appl. Chem.* **1985**, *57*, 603.
(42) Thommes, M.; Smarsly, B.; Groenewolt, M.; Ravikovitch, P. I.; Neimark, A. V. *Langmuir* **2006**, *22*, 756.
(43) Thommes, M.; Cychosz, K. *Adsorption* **2014**, *20*, 233.
(44) Jesson, D. E.; Pennycook, S. J. *Proc. R. Soc. London, Ser. A* **1995**, *449*, 273.
(45) ATTO 633, ATTO-Tec GmbH, 2015; https://www.atto-tec.com.
(46) Northrop, B. H.; Frayne, S. H.; Choudhary, U. *Polym. Chem.* **2015**, *6*, 3415.

DOI: 10.1021/jacs.5b10708
J. Am. Chem. Soc. 2016, 138, 1234−1239